Relationship between gain and Yb^{3+} concentration in Er^{3+}–Yb^{3+} doped waveguide amplifiers

Christof Strohhöfer[a] and Albert Polman
FOM Institute for Atomic and Molecular Physics, Kruislaan 407, 1098 SJ Amsterdam, The Netherlands

(Received 22 May 2001; accepted for publication 3 August 2001)

We have used a rate equation propagation model of an Er^{3+}/Yb^{3+} doped Al_2O_3 waveguide amplifier with copropagating pump at 980 nm to investigate the dependence of gain on Yb^{3+} concentration. The model includes excited state absorption and energy transfer upconversion processes within the Er^{3+} as well as the relevant energy transfer processes between Yb^{3+} and Er^{3+}. The results of the calculations indicate a close relationship of the parameters gain, launched pump power, waveguide length, and Yb^{3+} concentration. Codoping with a well-chosen Yb^{3+} concentration is shown to increase the gain around 1530 nm for all combinations of these parameters. The gain is improved most by Yb^{3+} codoping at pump powers around the amplifier threshold. At high pump powers the increase in gain of an Er^{3+}/Yb^{3+} doped waveguide is insignificant compared to that of its Er^{3+} doped counterpart. Furthermore for each launched pump power, a nonzero Yb^{3+} concentration can be determined, which maximizes the gain. © *2001 American Institute of Physics.*
[DOI: 10.1063/1.1406550]

I. INTRODUCTION

The triply charged ytterbium ion's strong absorption around 980 nm has made it an obvious candidate for use as a sensitizer for other luminescing ions. Codoping with Yb^{3+} has been shown to increase the photoluminescence or upconversion fluorescence emitted by the rare earth ions Pr^{3+}, Eu^{3+}, Tb^{3+}, Er^{3+}, and Tm^{3+}.[1–8] Even Cr^{4+} can be sensitized via Yb^{3+}.[9] The greater part of these studies has been made on codoping materials with Er^{3+} and Yb^{3+}, due to the Er^{3+} ion's relevance in optical amplifiers for telecommunication networks operating around 1550 nm. Sensitization in this case relies on the fact that the $^2F_{5/2}$ level of Yb^{3+} and the $^4I_{11/2}$ level of Er^{3+} are nearly resonant in energy. Due to its high absorption cross section, Yb^{3+} absorbs the pump radiation at 980 nm efficiently and can transfer this absorbed energy to Er^{3+}. This process is more power efficient than direct excitation of Er^{3+} in many materials, i.e., per incoming photon more Er^{3+} is excited.

This excitation scheme has been put to many different uses. Lasers operating in the wavelength window from 1530 to 1560 nm have been demonstrated.[10–12] In the area of optical telecommunications, fiber amplifiers and integrated optical amplifiers codoped with Er^{3+} and Yb^{3+} show gain at wavelengths around 1530 nm.[13–15]

Naturally, with the technology developed to this extent, great effort has gone into modeling Er^{3+}/Yb^{3+} doped amplifiers.[16–20] In this way, performance of a waveguide amplifier can be predicted based on the material it consists of and the waveguide configuration used. Obtaining accurate values for the relevant parameters of Er^{3+} and Yb^{3+} remains the central problem, and few results of the model calculations in the literature can be compared because of differing waveguide geometries.

Our purpose is to reach a qualitative understanding of the physics behind the dependence of the amplification in Er^{3+}/Yb^{3+} doped waveguide amplifiers on Yb^{3+} concentration. Part of this problem was already addressed in Ref. 16 for short fibers. We have chosen to investigate Al_2O_3 waveguides mainly for two reasons: first, gain has been reported in an Er^{3+} doped Al_2O_3 waveguide,[21] and we can use the respective waveguide cross section. Second, Al_2O_3 has been investigated in great detail with respect to Er^{3+} and Yb^{3+} doping,[22–24] so most—but not all—of the cross sections, decay rates, and energy transfer rates necessary as input to the model are known. For the purpose of this article, the unknown parameters have been filled in by comparison with similar materials.

This work is not aimed at making accurate predictions of the gain in the structure we have modeled. This would be impossible in view of the uncertainty in some of the material constants. We have therefore, for simplicity, also chosen to ignore amplified spontaneous emission (ASE). From the point of view of systems engineering this is of course a faux pas, since ASE is one of the major factors limiting amplifier performance. It leads to a reduction of the gain proportional to the average inversion in the waveguide and is therefore proportional to the gain itself.[25] However it does not influence the dependence of the gain features on Yb^{3+} concentration.

In the following we will briefly introduce the rate equations and the propagation model we have utilized to describe the Er^{3+}/Yb^{3+} doped waveguide amplifier. Subsequently, we will describe the results of our calculations and discuss their implications for the design of waveguide amplifiers.

[a]Author to whom correspondence should be addressed; electronic mail: c.strohhofer@amolf.nl

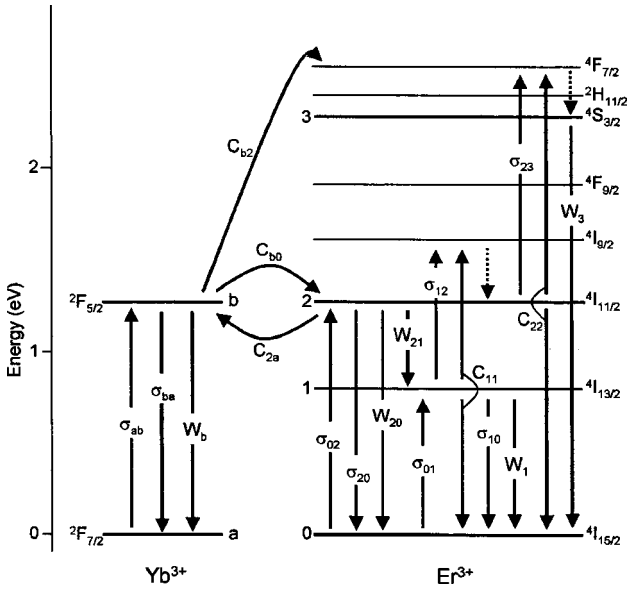

FIG. 1. Energy level diagram of Er^{3+} and Yb^{3+}. The arrows represent the processes included in the rate equation model used for the calculations. Included are absorption and stimulated emission processes σ_{ij}, spontaneous decays W_{ij}, and energy transfer processes C_{ij}. Dashed arrows represent spontaneous processes considered as instantaneous.

II. THE MODEL

We calculate the gain with a rate equation propagation model. The processes included in the model are depicted in Fig. 1. Absorption and stimulated emission processes are characterized by their respective cross sections σ_{if}, where i and f indicate the initial and final energy level of the process. Spontaneous decay is identified by its rate W_{if}. If no final level f is given, the corresponding decay rate W_i signifies the sum of all individual decay rates from level i to lower lying states.

A third kind of process included in the model is energy transfer between Yb^{3+} and Er^{3+} or between two excited Er^{3+} ions. These processes are characterized by their energy transfer rate constants C_{ij}. Here the subscripts i and j denote the energy levels populated prior to energy transfer. Furthermore all transitions indicated by dashed arrows in Fig. 1 are considered to be instantaneous.

The underlying assumption for this rate equation model to be valid is that excitation redistributes freely within both the Er^{3+} and the Yb^{3+} subsystems. This is the case when the concentration of the two ions is high enough to allow for energy migration.

The complete set of equations determining the population of the energy levels for this system is:

$$\frac{dN_b}{dt}=\sigma_{ab}\Phi_p N_a-\sigma_{ba}\Phi_p N_b-W_b N_b-C_{b0}N_b N_0 + C_{2a}N_a N_2-C_{b2}N_b N_2, \tag{1}$$

$$N_{\mathrm{Yb}}=N_a+N_b, \tag{2}$$

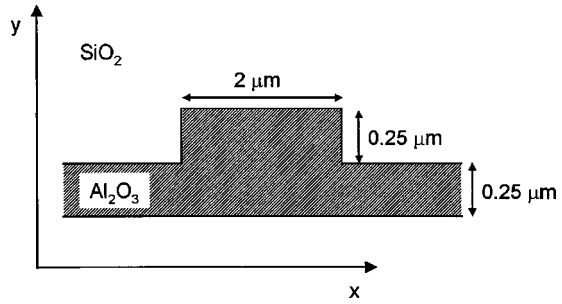

FIG. 2. Schematic cross section of the waveguide used for the calculations. A ridge structure of Al_2O_3 is embedded in SiO_2. The complete Al_2O_3 core is doped homogeneously with Er^{3+}, and Yb^{3+} if applicable. The narrow part of the Al_2O_3 structure extends to infinity in $+x$ and $-x$ directions. Note that the x and y axes have different scales.

$$\frac{dN_1}{dt}=\sigma_{01}\Phi_s N_0-\sigma_{10}\Phi_s N_1-\sigma_{12}\Phi_s N_1+W_{21}N_2-W_1N_1 - 2C_{11}N_1^2, \tag{3}$$

$$\frac{dN_2}{dt}=\sigma_{02}\Phi_p N_0-\sigma_{20}\Phi_p N_2+\sigma_{12}\Phi_s N_1-\sigma_{23}\Phi_p N_2 - W_2N_2+C_{11}N_1^2-2C_{22}N_2^2+C_{b0}N_bN_0 - C_{2a}N_aN_2-C_{b2}N_bN_2, \tag{4}$$

$$\frac{dN_3}{dt}=\sigma_{23}\Phi_p N_2-W_3N_3+C_{22}N_2^2+C_{b2}N_bN_2, \tag{5}$$

$$N_{\mathrm{Er}}=N_0+N_1+N_2+N_3. \tag{6}$$

In these equations N_i represents the population density of the energy level marked i in Fig. 1, with $i\in\{a,b,0,1,2,3\}$. Φ_p and Φ_s are the photon flux densities of the pump and signal radiation, respectively. These equations are solved for steady state at a given pump photon flux and for negligible signal photon flux (the so-called small-signal limit).

Figure 2 shows the cross section of the ridge waveguide we have assumed in these calculations. It is patterned after the waveguides fabricated in Refs. 21 and 23. It consists of an Al_2O_3 core, considered homogeneously doped with Er^{3+} and Yb^{3+} [indices of refraction $n(\lambda=1530\,\mathrm{nm})=1.65$ and $n(\lambda=980\,\mathrm{nm})=1.74$] surrounded by a thick cladding of SiO_2 [indices of refraction $n(\lambda=1530\,\mathrm{nm})=1.445$ and $n(\lambda=980\,\mathrm{nm})=1.451$]. The thick part of the waveguide has a width of 2μm and a thickness of 500 nm. Outside this central region, an Al_2O_3 film of 250 nm remains. The optical modes supported by this structure were calculated with a finite difference mode solver and approximated by two-dimensional Gaussian functions. Note that waveguides of this shape and size are single mode at 1530 nm but not at 980 nm. We have calculated the gain, assuming that only the fundamental mode at 980 nm is present in the waveguide. Including higher order modes at the pump wavelength will lead to a reduction of the gain of the system.[26]

We calculate the development of the power in pump and signal mode over the length of the waveguides. Pump and signal are copropagating. The optical power contained in the pump and signal modes is governed by

TABLE I. Parameters used for the numerical calculations.

Parameter	Symbol	Value	Source
Signal wavelength	λ_s	1530 nm	
Pump wavelength	λ_p	975 nm	
Er concentration	N_{Er}	3.35×10^{20} cm^{-3}	Ref. 23
Decay rate of Yb^{3+} $^2F_{5/2}$	W_b	1000 s^{-1}	unpublished measurement
Decay rate of Er^{3+} $^4I_{13/2}$	W_1	200 s^{-1}	Ref. 21
Decay rate of Er^{3+} $^4I_{11/2}$	W_2	30 000 s^{-1}	Ref. 21
Transition rate Er^{3+} $^4I_{11/2}\rightarrow{}^4I_{13/2}$	W_{21}	28 000 s^{-1}	cf. text
Decay rate of Er^{3+} $^4S_{3/2}$	W_3	100 000 s^{-1}	cf. text
Absorption cross section Yb^{3+} $^2F_{5/2}$ at λ_p	σ_{ab}	1.2×10^{-20} cm^2	Ref. 24
Emission cross section Yb^{3+} $^2F_{5/2}$ at λ_p	σ_{ba}	1.2×10^{-20} cm^2	Ref. 24
Absorption cross section Er^{3+} $^4I_{11/2}$ at λ_p	σ_{02}	2×10^{-21} cm^2	Ref. 24
Emission cross section Er^{3+} $^4I_{11/2}$ at λ_p	σ_{20}	2×10^{-21} cm^2	Ref. 24
Absorption cross section Er^{3+} $^4I_{13/2}$ at λ_s	σ_{01}	6×10^{-21} cm^2	Refs. 22 and 24
Emission cross section Er^{3+} $^4I_{13/2}$ at λ_s	σ_{10}	6×10^{-21} cm^2	Refs. 22 and 24
ESA cross section Er^{3+} $^4I_{13/2}$ at λ_s	σ_{12}	1×10^{-21} cm^2	Ref. 23, cf. text
ESA cross section Er^{3+} $^4I_{11/2}$ at λ_p	σ_{23}	0×10^{-21} cm^2	Ref. 30 and 31, cf. text
Energy transfer rate constant $Yb^{3+}\rightarrow Er^{3+}$ ($^2F_{5/2}+{}^4I_{15/2}\rightarrow{}^2F_{7/2}+{}^4I_{11/2}$)	C_{b2}	4×10^{-17} cm^3/s	Ref. 24
Energy transfer rate constant $Er^{3+}\rightarrow Yb^{3+}$ ($^4I_{11/2}+{}^2F_{7/2}\rightarrow{}^4I_{15/2}+{}^2F_{5/2}$)	C_{2b}	4×10^{-17} cm^3/s	cf. text
Energy transfer rate constant $Yb^{3+}\rightarrow Er^{3+}$ ($^2F_{5/2}+{}^4I_{11/2}\rightarrow{}^2F_{7/2}+{}^4F_{7/2}$)	C_{b3}	4×10^{-17} cm^3/s	cf. text
Cooperative upconversion coefficient Er^{3+}($^4I_{13/2}+{}^4I_{13/2}\rightarrow{}^4I_{9/2}+{}^4I_{15/2}$)	C_{11}	4×10^{-18} cm^3/s	Ref. 23
Cooperative upconversion coefficient Er^{3+}($^4I_{11/2}+{}^4I_{11/2}\rightarrow{}^4F_{7/2}+{}^4I_{15/2}$)	C_{22}	2×10^{-18} cm^3/s	Ref. 29, cf. text
Waveguide losses at λ_s	α_s	0.07 cm^{-1}	Ref. 34
Waveguide losses at λ_p	α_p	0.09 cm^{-1}	Ref. 34

$$\frac{dP_p(z)}{dz}=\frac{d}{dz}\int\int_{\text{core}}\Phi_p(x,y,z)\cdot h\nu_p\,dx\,dy$$

$$=\int\int_{\text{core}}\Phi_p(x,y,z)\cdot h\nu_p(-\sigma_{ab}N_a(x,y,z)+\sigma_{ba}N_b(x,y,z)-\sigma_{02}N_0(x,y,z)+\sigma_{20}N_2(x,y,z)$$

$$-\sigma_{23}N_2(x,y,z)-\alpha_p)dx\,dy, \tag{7}$$

$$\frac{dP_s(z)}{dz}=\frac{d}{dz}\int\int_{\text{core}}\Phi_s(x,y,z)\cdot h\nu_s\,dx\,dy$$

$$=\int\int_{\text{core}}\Phi_s(x,y,z)\cdot h\nu_s(-\sigma_{01}N_0(x,y,z)+\sigma_{10}N_1(x,y,z)-\sigma_{12}N_1(x,y,z)-\alpha_s)dx\,dy \tag{8}$$

In these relations, $h\nu_p$ and $h\nu_s$ are the energies of a pump and signal photon, respectively. α_p describes the waveguide scattering loss at the pump wavelength, and α_s at the signal wavelength. The position dependence of the population of the different energy levels is a consequence of its dependence on pump photon flux density, $N_i(x,y,z)=N_i(\Phi_p(x,y,z))$. The integral has to be evaluated in the Al_2O_3 part of the structure, since only this region is assumed to be doped with Er^{3+} and Yb^{3+}.

III. CHOICE OF THE PARAMETERS

The decay rates, absorption and emission cross sections, and energy transfer rate constants used as input in our calculations are based on measurements in Al_2O_3, as far as available. Many parameters, especially cross sections and ytterbium–erbium energy transfer rate constant, have become available only recently.[24] All parameters are listed in Table I. We will here comment on some of these parameters and make plausible our choice for those that have not yet been determined experimentally.

The energy transfer coefficient from Yb^{3+} to Er^{3+} is known to depend on ytterbium concentration for low concentrations, but is constant at high concentrations. Concentration dependent determination of C_{b0} in glasses[27] has shown that C_{b0} does not vary a lot for ytterbium concentrations higher than the minimum value we have used in the calculations ($N_{\text{Yb}}=3.35\times10^{20}$ cm^{-3}). It therefore seems reasonable to assume C_{b0} constant in our calculations. The energy back

transfer rate coefficient C_{2a} is very similar to C_{b0} in many materials.[6,28] We take $C_{2a}=C_{b0}$. The exact value of C_{2a} however has little influence on the numerical result because the population in the second excited state of Er^{3+} remains low even at high pump powers and therefore energy back transfer is not important. We also assume that $C_{b2}=C_{b0}$, since the broad emission spectrum of Yb^{3+} ensures a spectral overlap with the $^4F_{7/2}$ state comparable to that with the $^4I_{11/2}$ state. The assumption that the transition matrix elements involved in the energy transfer processes are equal is also reasonable. The transfer rate constant for cooperative upconversion processes from the Er^{3+} $^4I_{11/2}$ level, C_{22}, is unknown in Al_2O_3. Published data for this parameter in different materials show, however, that this coefficient is often close to $2\times10^{-18}\,cm^3/s$.[29] Therefore we have assumed this value to approximate C_{22} in Al_2O_3.

The excited state absorption cross section σ_{12} for radiation at 1530 nm from the $^4I_{13/2}$ state is also not known. We use the cross section for 1480 nm radiation instead.[23] Furthermore there are no data on excited state absorption originating from the $^4I_{11/2}$ level of Er^{3+} in Al_2O_3. In other crystalline materials such as yttrium–aluminum–garnet or $LiYF_4$ the relevant cross section σ_{23} at 980 nm is negligible.[30,31] A nonzero cross section will of course affect the population inversion between the $^4I_{13/2}$ state and ground state, however its influence is limited by the low population in the $^4I_{11/2}$ level and will become significant only for extremely high pump powers.

The branching ratio of the Er^{3+} $^4I_{11/2}$ state, which determines the rate W_{21}, is not known. However, it is known that the emission from the $^4I_{11/2}$ state to the ground state of around 980 nm is very weak compared to the transition originating from the $^4I_{13/2}$ level at 1530 nm. This fact has been taken into account through the choice of the value for $W_{21}\,(28\,000\,s^{-1})$. Finally there is no measured value available for the decay rate of the Er^{3+} $^4S_{3/2}$ state W_3 in Al_2O_3. It is generally fast compared to the decay rates of both the $^4I_{11/2}$ and $^4I_{13/2}$ states.[32,33] We choose $W_3=10^5\,s^{-1}$. As the branching ratio toward the ground state is high, most of the energy upconverted to this level is lost.

IV. RESULTS AND DISCUSSION

In the following paragraphs we will discuss the signal output from Er^{3+} doped ridge waveguides codoped with various concentrations of Yb^{3+}. We will try and elucidate the physical mechanisms behind these data. However we have to bear in mind that our model, with the peculiar cross section of the waveguide that has an Er^{3+}/Yb^{3+} doped region even at a large distance from the waveguide core (cf. Fig. 2), is not the simplest one possible from which to extract the physical principles. It is rather based on a structure realized experimentally, which has been reported to show gain under excitation at 1480 nm.[21] The optimal Er^{3+} concentration determined in the same series of work[21,23] $(3.35\times10^{20}\,cm^{-3})$ has been used as the starting point in our calculations.

A. Gain for a fixed waveguide length

Figure 3(a) shows the small-signal gain as a function of launched pump power at 980 nm for a fixed waveguide length of 8 cm. Plotted are results for several Yb^{3+} concentrations between 3.35×10^{20} and $26.8\times10^{20}\,cm^{-3}$, as well as for a waveguide doped only with Er^{3+}.

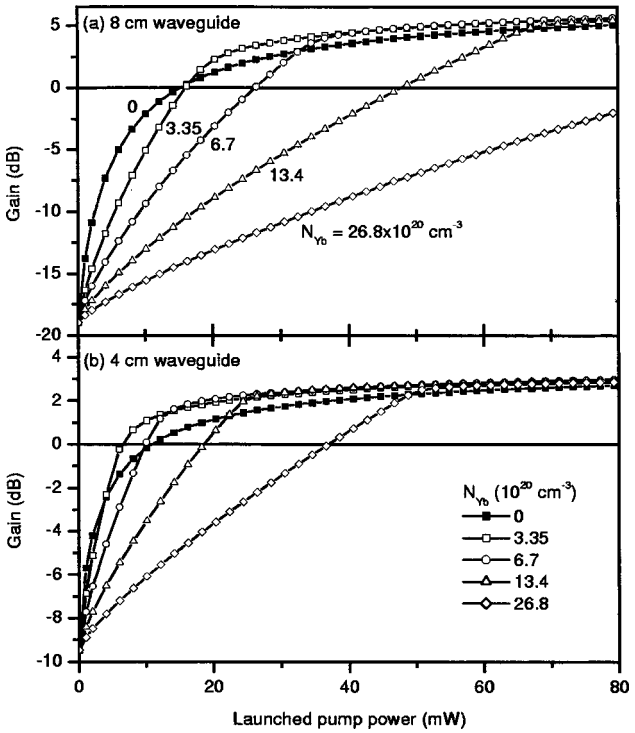

FIG. 3. Calculations of signal output from a waveguide of fixed length doped with $3.35\times10^{20}\,cm^{-3}$ Er^{3+} as a function of launched pump power. Different symbols represent different Yb^{3+} concentrations. Waveguide length: (a) 8 cm and (b) 4 cm.

At low pump powers the Er^{3+} is not inverted and most of the signal is absorbed. Increasing the pump power we first notice an effect on the signal output of the waveguide containing no Yb^{3+}. As the Yb^{3+} concentration is increased, the curves in Fig. 3(a) show a smaller initial increase with pump power. This behavior is caused by the higher absorption cross section of Yb^{3+} with respect to Er^{3+}, which limits the propagation of the pump through the waveguide and therefore the length over which the Er^{3+} is inverted. The gain at 1530 nm is determined by the difference in populations of the Er^{3+} $^4I_{13/2}$ and $^4I_{15/2}$ energy manifolds averaged over the waveguide length.

Increasing the pump power further will eventually enhance the signal leaving the Er^{3+}/Yb^{3+} doped waveguide over the signal leaving the Er^{3+} doped waveguide. This enhancement will take place at higher and higher pump powers as the Yb^{3+} concentration is increased. For very high pump powers, however, the signal output from all waveguides only depends on the Er^{3+} concentration and reaches the same value for all Yb^{3+} concentration. This is the limit of full inversion of all Er^{3+} ions in the waveguide.

Figure 3(b) shows the corresponding data for a waveguide of 4 cm length. The details of this graph are the same as described for Fig. 3(a), although shifted to lower pump power. This is to be expected as the total depletion of the pump is less in the shorter waveguide, resulting in a greater fraction of the Er^{3+} that is excited. However, the figure better

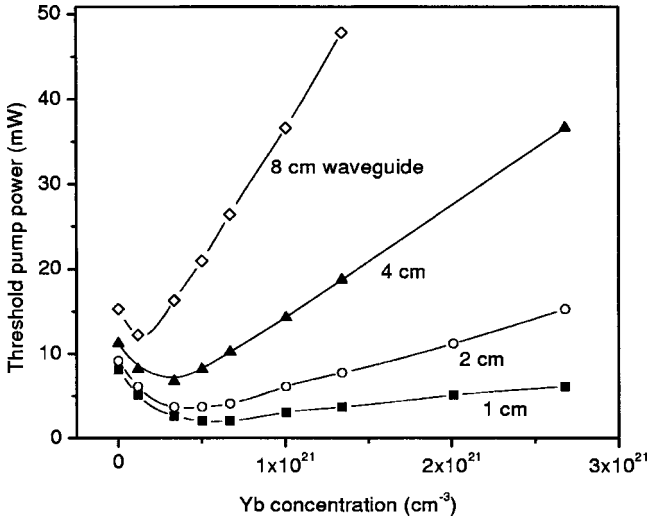

FIG. 4. The pump power threshold for net gain as a function of Yb^{3+} concentration for waveguides of different lengths. The drawn lines are guides to the eye. For increasing waveguide length, the minimum threshold power is achieved at decreasing Yb^{3+} concentration.

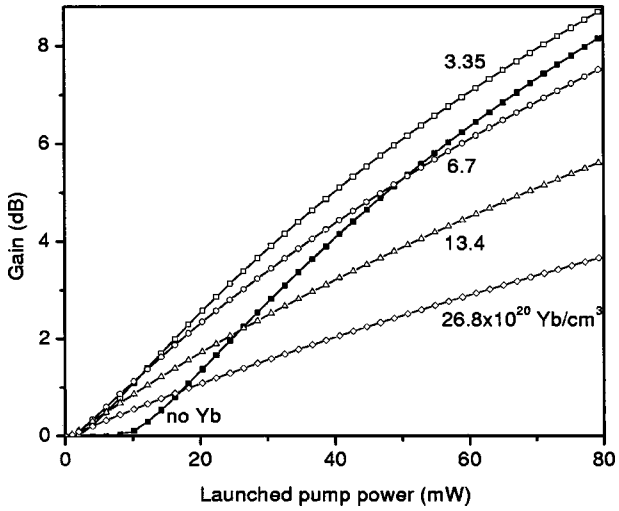

FIG. 5. Calculation of the maximum possible signal output from a waveguide doped with $3.35\times10^{20}\,cm^{-3}$ Er^{3+} as a function of launched pump power. Different symbols represent different concentrations of Yb^{3+}. The length of the waveguides has been adjusted for maximum gain for each Yb^{3+} concentration and each launched pump power.

illustrates the behavior at high pump powers, namely the output signal approaching its high pump power limit for all Yb^{3+} concentrations (the slight variations in gain at high pump powers reflect the differences in inversion of Er^{3+} in the tails of the signal mode).

The saturation at high pump power naturally follows from the energy transfer mechanism between Yb^{3+} and Er^{3+}. Considering the model depicted in Fig. 1 it is clear that the efficiency of the energy transfer from Yb^{3+} to Er^{3+} is limited by the transfer rate constant C_{2a} and the population in the Er^{3+} ground state (assuming for simplicity that W_2 is high, i.e., the population of the Er^{3+} $^4I_{11/2}$ state is negligible, we can neglect energy back transfer and energy transfer to higher lying states). This means that by increasing the launched pump power we will eventually reach a regime in which the excitation of Er^{3+} via Yb^{3+} can be neglected against its direct excitation. This is due both to the depletion of the ground state population of Er^{3+} and to the limitation on the energy transfer provided by the finite energy transfer rate constant, which is independent of pump power. If the amplifier is operated at such pump powers, Yb^{3+} codoping will only have a marginal effect (in our case only seen in the tails of the mode) and will be unnecessary.

On the other end of the power scale, there is however a rather clear correlation between gain threshold, length of the waveguide, and Yb^{3+} concentration. While for the 8 cm waveguide [Fig. 3(a)] the gain threshold for $N_{Yb}=0$ and $N_{Yb}=3.35\times10^{20}\,cm^{-3}$ nearly coincides, we see that for waveguides of 4 cm length concentrations of $N_{Yb}=3.35\times10^{20}\,cm^{-3}$ and $N_{Yb}=6.7\times10^{20}\,cm^{-3}$ have a lower gain threshold than the waveguide with no Yb^{3+}. For any length of the waveguide there is thus a corresponding Yb^{3+} concentration, which will decrease the threshold pump power to a minimum. This is shown in Fig. 4, which depicts the threshold pump power as a function of Yb^{3+} concentration for waveguides of different lengths. The minimum of the threshold power shifts to smaller and smaller Yb^{3+} concentrations for increasing waveguide length. This results from a tradeoff between the higher excitation efficiency of the Er^{3+} via Yb^{3+} and the depletion of the pump due to the high Yb^{3+} absorption cross section when propagating along the waveguide. When too much Yb^{3+} is added to the waveguide, the threshold for signal gain increases, the more rapidly, the longer the waveguide. Here we have chosen the gain threshold to demonstrate the dependence of pump power necessary to reach a certain gain level on Yb^{3+} concentration. Similar curves are obtained for any given signal output.

Returning to Fig. 3 we can see that the gain of an Er^{3+} doped waveguide amplifier is improved significantly by Yb^{3+} codoping only if it is operated at a pump power around its threshold, under the condition that the Yb^{3+} concentration is not too high. A high Yb^{3+} concentration therefore not only causes a high gain threshold, but also produces very little improvement in gain over the case with no Yb^{3+}. The effect of the large absorption of Yb^{3+} on the gain has to be taken into account when designing Er/Yb-doped waveguide amplifiers.

B. Maximum gain

In Fig. 5 we have plotted the results of calculations of the maximum gain as a function of launched pump power for several Yb^{3+} concentrations between 3.35×10^{20} and $26.8\times10^{20}\,cm^{-3}$. Additionally the calculated gain in a waveguide doped exclusively with Er^{3+} is depicted.

Each point in the plot represents a waveguide whose length is optimized for maximum gain at a given pump power. This means that the waveguide length is chosen such that at its end the transparency condition, an average inversion of zero over the cross section of the waveguide, is fulfilled. Consequently, the length of the waveguide differs for each of the points in the plot, both as a function of pump power for a given Yb^{3+} concentration, and as a function of Yb^{3+} concentration itself. Over the pump power range rep-

resented, the length of the waveguide without Yb^{3+} varies between 0 and 18 cm, and that of the waveguide doped with $26.8\times10^{20}\,Yb^{3+}/cm^3$ between 0 and 5.5 cm, to give an impression of the values involved.

There are several noteworthy points about this plot. First, the threshold injected pump power for gain decreases with increasing Yb^{3+} concentration. This is a consequence of the higher excitation probability of Er^{3+} via Yb^{3+} at low pump powers, which is caused by the high absorption cross section of Yb^{3+} and efficient energy transfer toward Er^{3+}.

Second, the slope of the curves, once the gain threshold is reached, decreases with increasing Yb^{3+} concentration. This is a signature of the higher conversion efficiency of absorbed pump photons for waveguides with smaller Yb^{3+} concentration. The lower the concentration of Yb^{3+}, the smaller the losses of pump energy caused by spontaneous decay of the Yb^{3+} ion. This feature becomes especially important for high inversion of the Er^{3+}, since in this case the probability is small that an excited Yb^{3+} ion can transfer its energy to an Er^{3+} ion in its ground state.

This also means that with increasing launched pump power, waveguides with higher Yb^{3+} concentration will eventually have less gain than waveguides with lower Yb^{3+} concentration. As a consequence, the maximum gain curves of waveguides with different Yb^{3+} concentrations will cross at a certain pump power. Several of these crossings can be seen in Fig. 5. Incidentally, the launched pump power at which these crossings occur should be independent of the inclusion of amplified spontaneous emission into the calculations, since ASE depends—to first order—on the total inversion in the waveguide. For equal gain, this total inversion has to be equal for the two waveguides involved.

It is clear from Fig. 5 that for any given launched pump power, a properly chosen nonzero Yb^{3+} concentration will increase the maximum gain achievable in the waveguide over the one without inclusion of Yb^{3+}. Although the curve given for a Yb^{3+} concentration of $3.35\times10^{20}\,cm^{-3}$ (open squares) will eventually run below the curve for zero Yb^{3+} concentration (solid squares) for launched pump powers of above 200 mW, decreasing the Yb^{3+} concentration further will shift the crossing toward even higher pump powers. Only in the academic case of infinite pump power/infinite waveguide length, the maximum gain cannot be increased by Yb^{3+} codoping. However, attention must be given to the fact that the energy transfer coefficients C_{ij} generally depend on concentration in this regime, and simple extrapolation cannot be applied. For all practical purposes, the launched pump power is limited to values of below 1 W, and Yb^{3+} codoping will always increase the maximum gain that can be achieved in a given waveguide. However, at high pump power this increase will be small.

Finally we would like to address the relation between Yb^{3+} concentration and launched pump power necessary to achieve a fixed gain (again for optimized length). This corresponds to a horizontal cut through Fig. 5 and has been plotted in Fig. 6 for clarity. The solid symbols give the pump power that has to be launched into the waveguide to reach a certain gain, as a function of the Yb^{3+} concentration in the waveguide. It can be discerned that the launched pump power is minimal for a finite Yb^{3+} concentration. This minimum moves to lower values of the Yb^{3+} concentration as the gain augments. This behavior follows directly from the argument made above about the concentration dependence of the maximum gain. It is once again a consequence of the tradeoff between excitation efficiency of the Er^{3+} via Yb^{3+} and the increased absorption in the waveguide caused by Yb^{3+}. If too high a Yb^{3+} concentration is chosen, the pump power needed to achieve a certain gain level rapidly increases.

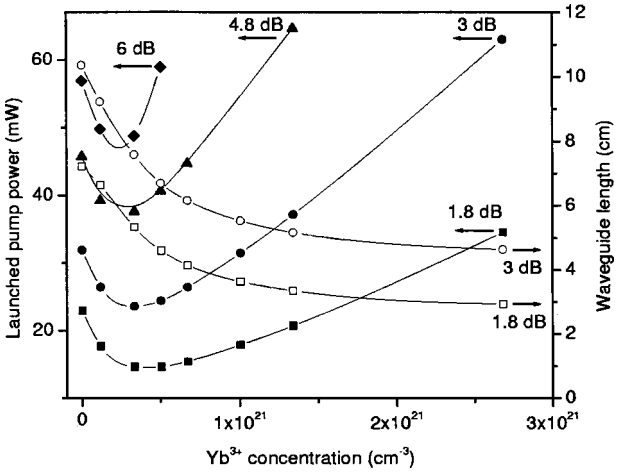

FIG. 6. Calculation of the pump power that has to be launched into the waveguide to reach a gain of 1.8, 3, 4.8, and 6 dB in a waveguide whose length has been optimized, as a function of Yb^{3+} concentration. Also plotted is the dependence of the waveguide length (optimized for maximum gain) on Yb^{3+} concentration for gains of 1.8 and 3 dB. The drawn lines are guides to the eye.

Included in Fig. 6 are two curves that show the development of waveguide length, at which a gain of 1.8 and 3 dB is achieved, as a function of Yb^{3+} concentration (open symbols). The waveguide length is a decreasing function of Yb^{3+} concentration, which reflects the increased absorption in the waveguide due to Yb^{3+}. Reducing the length of a waveguide amplifier by Yb^{3+} codoping may hold interest from a device design point of view, but it is clear that the penalty paid in pump power for a small reduction of waveguide length is large beyond the Yb^{3+} concentration at which the required pump power has its minimum (cf. Fig. 6). This is because the shorter waveguide length has to be offset by a gain in the tails of the mode, and therefore an oversupply of power in the central part of the waveguide. In materials in which excited state absorption of the pump radiation plays a role, this might actually have deleterious effects.

V. CONCLUSION

We have calculated the signal output from Al_2O_3 waveguides doped with Er^{3+} and Yb^{3+} with a rate equation propagation model. The behavior of the signal gain at 1530 nm was studied for an Er^{3+} concentration of $3.35\times10^{20}\,cm^{-3}$ and various Yb^{3+} concentrations between 3.35×10^{20} and $26.8\times10^{20}\,cm^{-3}$ and compared to that of a waveguide without Yb^{3+}.

We have investigated the relationship between gain and Yb^{3+} concentration, launched pump power, and waveguide length. In waveguides of fixed length, Yb^{3+} codoping can lower the gain threshold and increase the gain for launched pump powers around the threshold pump power. For pump powers above the point at which the direct excitation of Er^{3+} becomes as probable as its excitation via Yb^{3+}, the increase in gain over a waveguide doped only with Er^{3+} is small. The maximum gain that can be achieved in a waveguide amplifier for a fixed pump power can be increased by codoping with Yb^{3+}, if the concentration is chosen correctly. For each launched pump power, an optimized Yb^{3+} concentration can be determined. In the case where a certain gain has to be achieved, codoping with the right amount of Yb^{3+} substantially reduces the necessary pump power. However, we have found that doping the waveguides with high concentrations of Yb^{3+} always has detrimental effects on gain or pump power necessary to achieve a certain gain. This is due to an increased absorption of the pump and decreased absorbed photon conversion efficiency at high Yb^{3+} concentration. Where these effects set in depends on the exact values of the material parameters and the waveguide geometry.

In conclusion, our simulations have shown the need for careful optimization of the Yb^{3+} concentration in Er^{3+}/Yb^{3+} codoped waveguide amplifiers where pump and signal are copropagating. In applications using very high launched pump powers, it might be of advantage to grade the Yb^{3+} concentration along the length of the waveguide, or to only include it at the end of the waveguide, where the pump power is low enough so that Yb^{3+} increases the population inversion substantially.

ACKNOWLEDGMENTS

This work is part of the research program of the Foundation for Fundamental Research on Matter (FOM) and was financially supported by The Netherlands Organization for Scientific Research (NWO) and Symmorphix Inc.

[1] F. Auzel, Proc. IEEE **61**, 758 (1973).
[2] M. P. Hehlen, N. J. Cockroft, T. R. Gosnell, and A. J. Bruce, Phys. Rev. B **56**, 9302 (1997).
[3] R. H. Page *et al.*, J. Opt. Soc. Am. B **15**, 996 (1998).
[4] S. Tanabe, T. Kouda, and T. Hanada, Opt. Mater. **12**, 35 (1999).
[5] Y. Mita, T. Ide, M. Togashi, and H. Yamamoto, J. Appl. Phys. **85**, 4160 (1999).
[6] E. Cantelar, J. A. Muñoz, J. A. Sanz-García, and F. Cussó, J. Phys.: Condens. Matter **10**, 8893 (1998).
[7] J. Qiu, M. Shojiya, Y. Kawamoto, and K. Kadono, J. Lumin. **86**, 23 (2000).
[8] B.-C. Hwang *et al.*, J. Opt. Soc. Am. B **17**, 833 (2000).
[9] Y. G. Choi, H. K. Kim, Y. S. Han, and J. Heo, J. Mater. Res. **15**, 278 (2000).
[10] S. Taccheo, P. Laporta, and C. Svelto, Appl. Phys. Lett. **68**, 2621 (1996).
[11] M. Alouini, M. Brunel, F. Bretenaker, M. Vallet, and A. Le Floch, IEEE Photonics Technol. Lett. **10**, 1554 (1998).
[12] D. L. Veasey *et al.*, J. Non-Cryst. Solids **263&264**, 369 (2000).
[13] J. E. Townsend, W. L. Barnes, K. P. Jedrzejewski, and S. G. Grubb, Electron. Lett. **27**, 1958 (1991).
[14] P. F. Wysocki, N. Park, and D. DiGiovanni, Opt. Lett. **21**, 1744 (1996).
[15] D. Barbier *et al.*, IEEE Photonics Technol. Lett. **9**, 315 (1997).
[16] J. Nilsson, P. Scheer, and B. Jaskorzynska, IEEE Photonics Technol. Lett. **6**, 383 (1994).
[17] M. Federighi and F. Di Pasquale, IEEE Photonics Technol. Lett. **7**, 303 (1995).
[18] C. Lester, A. Bjarklev, T. Rasmussen, and P. G. Dinesen, J. Lightwave Technol. **13**, 740 (1995).
[19] M. Karásek, IEEE J. Quantum Electron. **33**, 1699 (1997).
[20] E. Cantelar, R. Nevado, G. Lifante, and F. Cussó, Opt. Quantum Electron. **32**, 819 (2000).
[21] G. N. van den Hoven *et al.*, Appl. Phys. Lett. **68**, 1886 (1996).
[22] G. N. van den Hoven *et al.*, Appl. Opt. **36**, 3338 (1997).
[23] G. N. van den Hoven *et al.*, J. Appl. Phys. **79**, 1258 (1996).
[24] C. Strohhöfer and A. Polman, Opt. Mater. (submitted).
[25] K. L. Shaklee, R. E. Nahory, and R. F. Leheny, J. Lumin. **7**, 284 (1973).
[26] M. V. D. Vermelho, U. Peschel, and J. S. Aitchison, J. Lightwave Technol. **18**, 401 (2000).
[27] V. P. Gapontsev and N. S. Platonov, ''Migration-accelerated quenching in glasses activated by rare-earth ions,'' in *Dynamical Processes in Disordered Systems*, edited by Y. M. Yen (Aedermannsdorf, Switzerland, 1989).
[28] C. Wyss, W. Lüthy, H. P. Weber, P. Rogin, and J. Hulliger, Opt. Commun. **144**, 31 (1997).
[29] P. M. Peters *et al.*, Appl. Opt. **38**, 6879 (1999).
[30] C. Labbé, J.-L. Doualan, S. Girard, R. Moncorgé, and M. Thuau, J. Phys.: Condens. Matter **12**, 6943 (2000).
[31] T. Danger *et al.*, J. Appl. Phys. **76**, 1413 (1994).
[32] P. Kabro *et al.*, J. Appl. Phys. **82**, 3983 (1997).
[33] M. Tsuda, K. Soga, H. Inoue, and A. Makishima, J. Appl. Phys. **88**, 1900 (2000).
[34] M. K. Smit, PhD thesis, Delft University of Technology, 1991.